

Inorganic–Organic Hybrids Formed by P,P'-Diphenylmethylenediphosphinate, pcp^{2-} , with the Cu^{2+} Ion. X-ray Crystal Structures of $[\text{Cu}(\text{pcp})(\text{H}_2\text{O})_2]\cdot\text{H}_2\text{O}$ and $[\text{Cu}(\text{pcp})(\text{bipy})(\text{H}_2\text{O})]$

Samuele Ciattini,[†] Ferdinando Costantino,[‡] Pablo Lorenzo-Luis,[§] Stefano Midollini,^{*,||} Annabella Orlandini,^{||} and Alberto Vacca[⊥]

Istituto di Chimica dei Composti Organometallici, Consiglio Nazionale delle Ricerche, Via Madonna del Piano, 50019 Sesto Fiorentino, Firenze, Italy, Centro di Cristallografia e Dipartimento di Chimica, Università di Firenze, Via della Lastruccia 3, 50019 Sesto Fiorentino, Firenze, Italy, Dipartimento di Chimica, Università di Perugia, Via Elce di Sotto 8, 06123 Perugia, Italy, and Departamento de Química Inorgánica, Universidad de La Laguna, E-38200 Tenerife, Canary Islands, Spain

Received February 1, 2005

Weakly coordinated $[\text{Cu}(\text{pcp})(\text{H}_2\text{O})_n]$ complexes are formed in aqueous solution, at room temperature, by interaction of P,P'-diphenylmethylenediphosphinic acid (H_2pcp) with copper(II) ions. However, heating of the solutions gives rise to the formation of two extended metal–oxygen networks of formulas $[\text{Cu}(\text{pcp})(\text{H}_2\text{O})_2]\cdot\text{H}_2\text{O}$, **1**, and $[\text{Cu}(\text{pcp})(\text{H}_2\text{O})_2]$, **2**. In the presence of 2,2'-bipyridyl (bipy) the diamine derivative $[\text{Cu}(\text{pcp})(\text{bipy})(\text{H}_2\text{O})]$, **4**, has been isolated. Complex **1** easily loses water to form a monohydrated derivative $[\text{Cu}(\text{pcp})(\text{H}_2\text{O})]$, **3**, whereas **2** is completely dehydrated after prolonged heating at 150 °C, under vacuum. The compounds **1** and **2** have substantially different solid-state structures as shown by X-ray powder diffraction spectra, IR spectra, and thermogravimetric analyses. Consistently, the two complexes cannot be directly interconverted and present different dehydration pathways. Rehydration of these materials in both cases allows quantitative formation of **1**. X-ray analysis established that the structure of **1** consists of a corrugated two-dimensional layered polymeric array, where infinite zigzag chains of Cu centers and bridging phenylphosphinate ligands are linked together through strong hydrogen-bonding interactions; the structure of **4** consists of monodimensional polymers, where the hydrogen-bonding interactions play an essential bridging role in the extended architecture. In both structures the metal center displays a five-coordinate environment with approximate square pyramidal geometry, with the pcp ligand acting as bidentate and monodentate in **1** and solely as bidentate in **4**. In **1** the coordination sphere is completed through water molecules; in **4**, through water and diamine ligands. The thermogravimetric analyses of the complexes are compared with those of the related hybrids $[\text{M}(\text{pcp})(\text{H}_2\text{O})_3]\cdot\text{H}_2\text{O}$, where M = Mn, Co, or Ni, confirming that noncoordinated water molecules also play a basic role in determining the molecular packing.

Introduction

Inorganic–organic hybrids are materials of intense interest in the field of contemporary material chemistry, as these materials could exhibit attractive properties such as zeolite

characteristics, catalytic activity, relevant magnetism, and nonlinear optical behavior.^{1,2}

A large variety of ligands containing bridging functionalities such as carboxylates [see examples in refs 3–5] and/or phosphonates [see examples in refs 6–9] have been

* To whom correspondence should be addressed. E-mail: stefano.midollini@iccom.cnr.it.

[†] Centro di Cristallografia, Università di Firenze.

[‡] Università di Perugia.

[§] Universidad de La Laguna.

^{||} CNR.

[⊥] Dipartimento di Chimica, Università di Firenze.

(1) Hagrman, P. J.; Hagrman, D.; Zubieta, J. *Angew. Chem., Int. Ed.* **1999**, *38*, 2639.

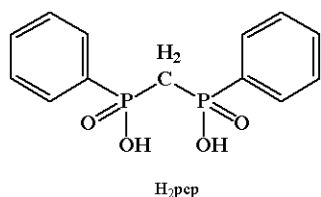
(2) Allcock, H. R. *Adv. Mater.* **1994**, *6*, 106.

(3) Pan, L.; Lin H.; Lei, X.; Huang, X.; Olson, D. H.; Turro, N. J.; Li, J. *Angew. Chem., Int. Ed.* **2003**, *42*, 542.

(4) Livage, C.; Egger, C.; Ferey, G. *Chem. Mater.* **2001**, *13*, 410.

(5) Forster, P. M.; Thomas, P. M.; Cheetham, A. K. *Chem. Mater.* **2002**, *14*, 17.

Chart 1



successfully employed in recent years to synthesize extended networks with metal ions. Differently related phosphinate ligands have been comparatively less investigated,^{10,11} and these have been generally found to favor the formation of monodimensional polymers. However, phosphinates appear to be interesting ligands in inorganic–organic hybrids engineering. Even if the phosphinate group contains only two oxygen donor atoms, the presence of two organic moieties should allow a better modulation of the structure of the resulting metal complexes than in the case of the related phosphonate.

Recently we have found that the bifunctional dianion of the *P,P'*-diphenylmethylenediphosphinic acid (H_2pcp)¹² (Chart 1) possesses interesting coordinating characteristics to give extended networks. Indeed, pcp^{2-} can bridge metal ions with formation of six-membered chelate rings, each oxygen atom in turn being able to bridge two metal centers. Moreover, the diphosphinate can balance the charge of a bivalent metal cation, avoiding the presence of counteranions. When the phosphinate oxygen atoms are not capable of saturating the metal center, water molecules are in turn coordinated, potentially causing the formation of a net of hydrogen bonds. Actually extended networks of $\text{Be}(\text{II})$,¹³ $\text{Mn}(\text{II})$, $\text{Co}(\text{II})$, $\text{Ni}(\text{II})$,¹⁴ $\text{Zn}(\text{II})$,¹⁵ and $\text{Pb}(\text{II})$ ¹⁶ with this ligand have been reported.

The $[\text{M}(\text{pcp})(\text{H}_2\text{O})_3]\cdot\text{H}_2\text{O}$ ($\text{M} = \text{Mn}, \text{Co}, \text{and Ni}$)¹⁴ hybrids, containing ions octahedrally coordinated, represent an isomorphous series, where the overall structure is arranged in the form of corrugated two-dimensional (2D) layers. As a consequence, in such a series the metal can be replaced by another metal without changing the primary structure, and mixed-metal pcp complexes could be isolated. Remarkable in these networks is the role of the water molecules, both of coordination and of crystallization, which are involved in

intricate hydrogen-bonding networks and are able to cement molecules and chains in more extended structures. The importance of the building role of the water molecules is well exemplified in the recently reported $\text{Be}(\text{pcp})(\text{H}_2\text{O})_2$ derivative.¹³ Here the pcp^{2-} ligand acts as bidentate, whereas the cement of the extended network is constituted by the hydrogen bonding between the coordinated water molecules and the PO_2 oxygen atoms not involved in direct bonding to the beryllium ion. The architecture is different in the pcp hybrids with $\text{Zn}(\text{II})$ ¹⁵ and $\text{Pb}(\text{II})$,¹⁶ where the water molecules are absent and the polymeric arrangement [one-dimensional (1D) for Pb and 2D for Zn] is reached through bridging oxygen atoms of the phosphinate ligand.

Now here we report the synthesis and characterization of the hydrated copper(II) complexes $[\text{Cu}(\text{pcp})(\text{H}_2\text{O})_2]\cdot\text{H}_2\text{O}$ (**1**), $[\text{Cu}(\text{pcp})(\text{H}_2\text{O})_2]$ (**2**), and $[\text{Cu}(\text{pcp})(\text{H}_2\text{O})]$ (**3**) and also of the diamine derivative $[\text{Cu}(\text{pcp})(\text{bipy})\text{H}_2\text{O}]$ (**4**). The molecular structures of **1** and **4** have been determined by single-crystal diffraction analyses, whereas no suitable crystals were available for compounds **2** and **3**. The thermogravimetric analyses of these copper pcp complexes have been compared with those of the previously reported manganese, cobalt, and nickel derivatives.

Experimental Section

Materials and Methods. All chemicals were used as purchased without purification. $\text{H}_2(\text{pcp})$ was prepared as previously described¹² and then purified by recrystallization from ethanol.

IR spectra were recorded, as Nujol mulls, on a Perkin-Elmer 1600 series FTIR spectrometer. Thermal analyses (TG-DTA) were carried out on a Perkin-Elmer Diamond TG-DTA system (SEGAI Service of the University of La Laguna), under a nitrogen atmosphere (flow rate $80 \text{ cm}^3\cdot\text{min}^{-1}$) in the range from ambient temperature to $550 \text{ }^\circ\text{C}$. Small needlelike crystals of the samples (between 6.258 and 3.039 mg) were heated in an aluminum crucible ($45 \mu\text{L}$) at a rate of $10 \text{ }^\circ\text{C}\cdot\text{min}^{-1}$. The TG curves were analyzed as mass loss (milligrams) as a function of temperature. The numbers of decomposition steps were identified by use of derivative thermogravimetric curves (DTG). The DTA curves were analyzed by differential thermal analysis [ΔT (microvolts)]. X-ray powder diffraction patterns were collected by the step scanning procedure with $\text{Cu K}\alpha$ radiation on a Philips X'PERT APD diffractometer, PW3020 goniometer equipped with a bent graphite monochromator on the diffracted beam. Divergence and scatter slits (0.5°) and a 0.1 mm receiving slit were used. The LFF ceramic tube operated at 40 kV and 30 mA. To minimize preferred orientations, the sample was carefully side-loaded onto an aluminum sample holder with an oriented quartz monocrystal underneath. The effective magnetic moments were measured, at room temperature, on a Cryogenics S600 SQUID magnetometer. The determination of the equilibrium constants was performed from pHmetric titrations at 298 K at an ionic strength of 0.5 mol dm^{-3} in Me_4NCl by use of the HYPERQUAD program.¹⁷ The emf apparatus and the experimental technique have been described previously.¹⁸ The titrations were carried out by adding a 0.1 mol dm^{-3} Me_4NOH solution to acid solutions containing either the ligand (deprotonation experiments)

- (6) Bakhmutova, E. V.; Ouyang, X.; Medvedev, D. G.; Clearfield, A. *Inorg. Chem.* **2003**, *42*, 7046.
- (7) Kong, D.; Li, Y.; Ross Jr., J. H.; Clearfield, A. *Chem. Commun.* **2003**, 1720.
- (8) Stock, N.; Frey, S. A.; Stucky, G. D.; Cheetham, A. K. *J. Chem. Soc., Dalton Trans.* **2000**, 4292.
- (9) Burlholder E.; Golub, V. O.; O'Connor, C. J.; Zubieta, J. *Inorg. Chim. Acta* **2002**, *340*, 127.
- (10) Grohol, D.; Ginge, F.; Clearfield, A. *Inorg. Chem.* **1999**, *38*, 751.
- (11) Oliver, K. W.; Rettig, S. J.; Thomson, R. C.; Trotter, J.; Xuia, S. *Inorg. Chem.* **1997**, *36*, 2465.
- (12) Garst, M. E. *Synth. Commun.* **1979**, *9*, 261.
- (13) Ceconi, F.; Dominguez, S.; Masciocchi, N.; Midollini, S.; Sironi, A.; Vacca, A. *Inorg. Chem.* **2003**, *42*, 2350.
- (14) Berti, E.; Ceconi, F.; Ghilardi, C. A.; Midollini, S.; Orlandini, A.; Pitzalis, E. *Inorg. Chem. Commun.* **2002**, *5*, 1041.
- (15) Ceconi, F.; Dakternieks, D.; Duthie, A.; Ghilardi, C. A.; Gili, P.; Lorenzo-Luis, P. A.; Midollini, S.; Orlandini, A. *J. Solid State Chem.* **2004**, *177*, 786.
- (16) Ceconi, F.; Ghilardi, C. A.; Midollini, S.; Orlandini, A. *Inorg. Chem. Commun.* **2003**, *6*, 546.

- (17) Gans, P.; Sabatini, A.; Vacca, A. *Talanta* **1996**, *43*, 1739.
- (18) Alderighi, L.; Vacca, A.; Ceconi, F.; Midollini, S.; China, E.; Dominguez, S.; Valle, A.; Dakternieks D.; Duthie, A. *Inorg. Chim. Acta* **1999**, *285*, 39.

Table 1. Crystal Data and Structure Refinement for **1** and **4**

	1	4
empirical formula	C ₁₃ H ₁₈ Cu ₁ O ₇ P ₂	C ₂₃ H ₂₂ Cu ₁ N ₂ O ₅ P ₂
formula weight	411.75	531.91
temperature (K)	293(2)	293(2)
wavelength (Å)	1.541 80	0.710 69
crystal system, space group	monoclinic, <i>P2/c</i>	triclinic, <i>P-1</i>
unit cell dimensions		
<i>a</i> (Å)	19.490(8)	7.135(9)
<i>b</i> (Å)	9.443(3)	10.870(2)
<i>c</i> (Å)	9.434(3)	16.271(5)
α (deg)	90	99.26(2)
β (deg)	110.37(3)	99.94(6)
γ (deg)	90	102.10(5)
volume (Å ³)	1627.7(10)	1189.7(16)
Z, calcd density (g cm ⁻³)	4, 1.680	2, 1.485
absorption coefficient (mm ⁻¹)	4.064	1.089
<i>F</i> (000)	844	546
crystal size (mm)	0.45 × 0.40 × 0.012	0.40 × 0.125 × 0.05
θ range for data collection (deg)	4.68–55.07	2.56–22.97
limiting indices	−20 ≤ <i>h</i> ≤ 19, 0 ≤ <i>k</i> ≤ 10, 0 ≤ <i>l</i> ≤ 10	−7 ≤ <i>h</i> ≤ 7, −11 ≤ <i>k</i> ≤ 11, 0 ≤ <i>l</i> ≤ 17
reflections collected/unique	2347/1904	3490/3288
refinement method	full-matrix least-squares on <i>F</i> ²	full-matrix least-squares on <i>F</i> ²
data/restraints/parameters	1904/0/208	3288/0/386
goodness-of-fit on <i>F</i> ²	0.990	1.023
final <i>R</i> indices [<i>I</i> > 2σ(<i>I</i>)]	<i>R</i> 1 = 0.0660, w <i>R</i> 2 = 0.1562	<i>R</i> 1 = 0.0414, w <i>R</i> 2 = 0.0954
<i>R</i> indices (all data)	<i>R</i> 1 = 0.0877, w <i>R</i> 2 = 0.1689	<i>R</i> 1 = 0.0710, w <i>R</i> 2 = 0.1063
largest diff. peak, hole (e ⁻ Å ⁻³)	0.744, −0.466	0.385, −0.511

or a metal chloride (CoCl₂, NiCl₂, and CuCl₂ in the complex formation experiments). Concentrations of metal and ligand were in the range 1–3 mmol dm⁻³. The ligand-to-metal ratios were 1:1 and 2:1 (two titrations, 60–90 data points in the pH range 2.5–5.5). At higher pH regions, precipitation of metal-containing species (presumably metal hydroxides) occurred and this precluded further collection of data. The electrode system was calibrated in terms of hydrogen ion concentration [H⁺], by the method of Gran.¹⁹

Synthesis of [Cu(pcp)(H₂O)₂]-H₂O, **1.** H₂pcp (0.1 g, 0.34 mmol) was dissolved in water (65 mL) at room temperature under stirring (ca. 1 h). A solution of copper(II) acetate monohydrate (0.068 g, 0.34 mmol) in 10 mL of water was added. The resulting solution was evaporated at ca. 70 °C till pale sky-blue crystals precipitated. The complex was filtered, washed with water, and dried in air at room temperature. Yield 0.120 g, 86%. Anal. Calcd for C₁₃H₁₈-Cu₁O₇P₂: C, 37.92; H, 4.41. Found: C, 37.63; H, 4.20. μ_{eff} = 1.93μ_B at 295 K.

Synthesis of [Cu(pcp)(H₂O)₂], **2.** H₂pcp (0.1 g, 0.34 mmol) was dissolved in 65 mL of boiling water, and then a solution of copper(II) acetate monohydrate (0.068 g, 0.34 mmol) in 10 mL of water was added. The resulting solution was concentrated by boiling till thin pale-blue crystals precipitated. The resulting mixture was cooled at room temperature; then the compound was filtered, washed with water, and dried in air. Yield 0.108 g, 81%. Anal. Calcd for C₁₃H₁₆-Cu₁O₆P₂: C, 39.65; H, 4.09. Found: C, 39.28; H, 4.04. The complex, held under vacuum (5 × 10⁻² Torr) at 150 °C for 3 days, loses water to yield an amorphous material analyzing as Cu(pcp). Anal. Calcd for C₁₃H₁₂CuO₄P₂: C, 43.65; H, 3.38. Found: C, 43.50; H, 3.45.

Synthesis of [Cu(pcp)(H₂O)], **3.** The solid complex **1**, at room temperature, slowly loses water till after ca. 20 days it analyzes as Cu(pcp)(H₂O). This compounds can be obtained more rapidly (hours) by heating **1**, in air, at temperatures > 70 °C. Alternatively, the monohydrated derivative can be obtained by washing **1** with ethanol. The composition of monohydrated solid does not change

by further heating at 150 °C, under vacuum (5 × 10⁻² Torr). Anal. Calcd for C₁₃H₁₄Cu₁O₅P₂: C, 41.55; H, 3.76. Found: C, 41.47; H, 3.61.

Synthesis of [Cu(pcp)(bipy)(H₂O)], **4.** [Cu(pcp)(H₂O)₂](H₂O) (0.050 g, 0.12 mmol) was suspended in 50 mL of boiling water, then solid 2,2'-bipyridyl (0.019 g, 0.12 mmol) was added. The complex dissolved to give a blue solution, which was filtered and concentrated at 70–80 °C till blue crystals precipitated. The complex was filtered, washed with water, and dried in air at room temperature. Yield 0.051 g, 80%. Alternatively, the complex can be obtained by reacting in water equimolar amounts of H₂pcp, Cu-(acetate)₂·H₂O, and bipy at 70–80 °C. Anal. Calcd. for C₂₃H₂₂-Cu₁N₂O₅P₂: C, 51.93; H, 4.17; N, 5.27. Found: C, 51.68; H, 4.12; N, 5.24. μ_{eff} = 1.90μ_B at 295 K.

X-ray Data Collection and Structure Solution. Diffraction data for **1** and **4** derivatives were collected at room temperature on a Philips PW1100 and on an Enraf Nonius CAD4 automatic diffractometer, respectively. Unit cell parameters for both compounds were determined by least-squares refinement of the setting angles of 25 carefully centered reflections. Crystal data and data collection details of **1** and **4** are given in Table 1. The intensities *I* were assigned the standard deviations σ(*I*) calculated by using a value of 0.03 for the instability factor *k*.²⁰ They were corrected for Lorentz polarization effects and for absorption.²¹ Atomic scattering factors for neutral atoms were taken from ref 22. Both Δ*f*' and Δ*f*'' components of anomalous dispersion were included for all non-hydrogen atoms.²³ The structures were solved by direct methods and refined by full-matrix *F*² refinement, with anisotropic thermal parameters assigned to all non-hydrogen atoms. Whereas in **1** the hydrogen atoms were introduced in their calculated positions riding on their carbon atoms,

(19) Gran, G. *Analyst* **1952**, *77*, 661.

(20) Corfield, P. W. R.; Doedens, R. J.; Ibers, J. A. *Inorg. Chem.* **1967**, *6*, 197.

(21) Parkin, S.; Moezzi, B.; Hope, H. *J. Appl. Crystallogr.* **1995**, *28*, 53.

(22) *International Tables for X-ray Crystallography*; Kluwer: Dordrecht, The Netherlands, 1992; Vol. C, p 500.

(23) *International Tables for X-ray Crystallography*; Kluwer: Dordrecht, The Netherlands, 1992; Vol. C, p 219.

Table 2. Decimal Logarithm Values of the Equilibrium Constants for the Reactions of pcp^{2-} with H^+ , Co^{2+} , Ni^{2+} , and Cu^{2+} in Aqueous Solution^a

reaction	log <i>K</i>
$\text{H}^+ + \text{pcp}^{2-} \rightleftharpoons \text{Hpcp}^-$	3.33(1)
$\text{H}^+ + \text{Hpcp}^- \rightleftharpoons \text{H}_2\text{pcp}$	1.35(9)
$\text{Co}^{2+} + \text{pcp}^{2-} \rightleftharpoons \text{Copcpc}$	2.9(1)
$\text{Ni}^{2+} + \text{pcp}^{2-} \rightleftharpoons \text{Nipcp}$	3.43(6)
$\text{Cu}^{2+} + \text{pcp}^{2-} \rightleftharpoons \text{Cupcp}$	4.25(9)

^a $T = 298 \text{ K}$ and $I = 0.5 \text{ mol dm}^{-3}$, Me_4NCl . Values in parentheses are standard deviations on the last significant figure.

with thermal parameters 20% larger, in **4** it was possible to locate the hydrogen atoms from a difference Fourier map and refine them. The function minimized during the refinement was $\sum w(F_o^2 - F_c^2)^2$, with $w = 1/[\sigma^2(F_o^2) + (0.0876P)^2 + 11.24P]$ and $w = 1/[\sigma^2(F_o^2) + (0.0636P)^2]$ [$P = (\max(F_o^2, 0) + 2F_c^2)/3$] for **1** and **4**, respectively. All the calculations were performed on a Pentium processor, using the package WINGX²⁴ (SIR97,²⁵ SHELX97,²⁶ ORTEP-III²⁷).

Results and Discussion

Interaction of Copper(II) Ions with H_2pcp in Aqueous Solution and Synthesis of Solid Networks. The interaction of H_2pcp with copper(II) ions in aqueous solution has been investigated by potentiometric measurements. The results of the experimental data are shown in Table 2 together with those of the related cobalt(II) and nickel(II) complexes for comparison purposes. The two basicity constants of pcp^{2-} were in excellent agreement with a recent determination under the same experimental conditions ($\log K = 3.34$ and 1.3, respectively).¹³ The complex formation experiments were all satisfactorily fitted with the assumption that only one complex species (namely ML) is present at the equilibrium. The characterized complexes appear to be relatively weak at room temperature. This is probably the reason complex species with higher ligand-to-metal ratios were not detected under the experimental conditions of this study; in any case, the trend of the stability $\text{Co(II)} < \text{Ni(II)} < \text{Cu(II)}$ is that expected according to the Irving–Williams order.

However, we have found that, in agreement with previous reports,²⁸ the increasing temperature favors the elimination of coordinated water and the formation of infinite metal–oxygen networks. As a matter of fact, heating of the aqueous solution of copper(II) acetate [the complexes can be prepared also from copper(II) nitrate with similar yields] and H_2pcp allows the preparation of two polymeric complexes. At ca. 70 °C, pale blue crystals of formula $\text{Cu}(\text{pcp})(\text{H}_2\text{O})_3$ were isolated, whereas from a boiling solution, thin crystals of the same color but analyzing as $\text{Cu}(\text{pcp})(\text{H}_2\text{O})_2$ precipitated. The IR spectra of the two compounds (Figure 1) appear to be rather similar, even if the spectrum of $\text{Cu}(\text{pcp})(\text{H}_2\text{O})_3$

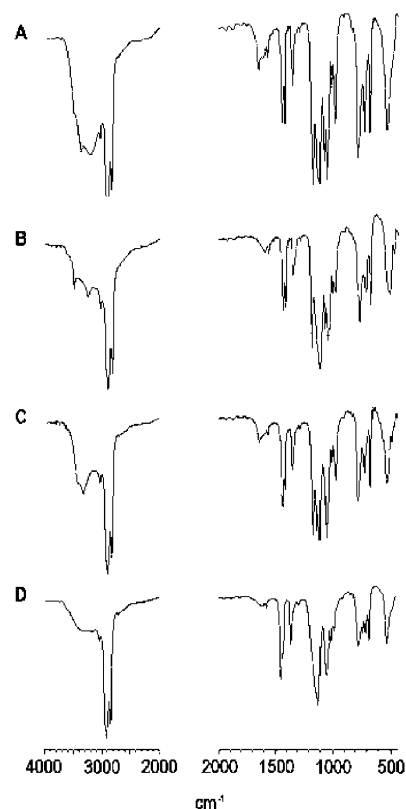


Figure 1. IR spectra of the complexes (A) $\text{Cu}(\text{pcp})(\text{H}_2\text{O})_3$, (B) $\text{Cu}(\text{pcp})(\text{H}_2\text{O})_2$, (C) $\text{Cu}(\text{pcp})(\text{H}_2\text{O})_2$, and (D) $\text{Cu}(\text{pcp})$ [material from $\text{Cu}(\text{pcp})(\text{H}_2\text{O})_2$ at 150 °C under vacuum].

shows three O–H stretching bands of H_2O at 3540 (m), 3391 (s), and 3206 (s, br), whereas that of $\text{Cu}(\text{pcp})(\text{H}_2\text{O})_2$ shows in the same region two bands at 3394 (m) and 3339 (s). It is noteworthy that this latter complex, even if treated with water for days at room temperature, remains absolutely unchanged. On the other hand, the complex $\text{Cu}(\text{pcp})(\text{H}_2\text{O})_3$ slowly darkens in air, at room temperature (from pale blue to sky blue), losing water to give, in ca. 20 days, a derivative analyzing as $\text{Cu}(\text{pcp})(\text{H}_2\text{O})$. The same material can be rapidly obtained by either heating $\text{Cu}(\text{pcp})(\text{H}_2\text{O})_3$ at 150 °C (0.5 h) or washing the same with ethanol. The solid $\text{Cu}(\text{pcp})(\text{H}_2\text{O})$ remains substantially unchanged after further heating, under vacuum (5×10^{-2} Torr), at 150 °C for 3 days. Its IR spectrum shows a new pattern in the ν_{OH} range (Figure 1) with two bands at 3510 and 3272 cm^{-1} . It is noteworthy that this latter derivative, when treated with water at room temperature, quantitatively re-forms the trihydrated compound (IR and analysis). The process can be repeated without any decomposition. By contrast, the treatment of complex $\text{Cu}(\text{pcp})(\text{H}_2\text{O})_2$ at 150 °C, under vacuum (5×10^{-2} Torr), allows a progressive dehydration as shown by the IR spectra where the water stretching absorptions progressively disappear. In Figure 1D is reported the IR spectrum of the material $\text{Cu}(\text{pcp})$ resulting after heating of $\text{Cu}(\text{pcp})(\text{H}_2\text{O})_2$ at 150 °C under vacuum for 3 days. Also, this latter solid, when reacted with water at room temperature, gives the trihydrate complex $\text{Cu}(\text{pcp})(\text{H}_2\text{O})_3$. All these findings are summarized in Scheme 1.

(24) Farrugia, L. J. *J. Appl. Crystallogr.* **1999**, *32*, 876.

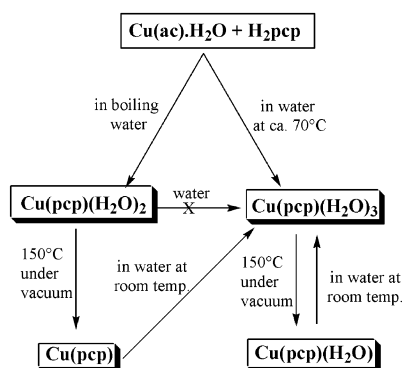
(25) Altomare, A.; Burla, M. C.; Camalli, M.; Cascarano, G. L.; Giacovazzo, C.; Guagliardi, A.; Moliterni, A. G. C.; Polidori, G.; Spagna, R. *J. Appl. Crystallogr.* **1999**, *32*, 115.

(26) Sheldrick, G. M. *SHELX97*; University of Göttingen: Göttingen, Germany, 1997.

(27) Burnett, M. N.; Johnson, C. K.; *ORTEP-III*; Oak Ridge National Laboratory: Oak Ridge, TN, 1996.

(28) Livage, C.; Egger, C.; Ferey, G. *Chem. Mater.* **2001**, *13*, 410.

Scheme 1



The X-ray powder diffraction spectra of $\text{Cu(pcp)(H}_2\text{O)}_3$ and $\text{Cu(pcp)(H}_2\text{O)}_2$ are shown in Figure 2. The diffraction pattern for $\text{Cu(pcp)(H}_2\text{O)}$ is not shown because it contains only a few weak signals, the compound being practically amorphous. The position of the reflections for the pattern of $\text{Cu(pcp)(H}_2\text{O)}_3$ are in agreement with the cell parameters derived from the single-crystal X-ray analysis, but the basal reflections ($h00$) are strongly enhanced, probably because of severe orientation effects.²⁹ The XRD pattern of **2** has been indexed by use of the TREOR program,³⁰ giving as the best solution the tetragonal cell $a = 9.1887$ and $c = 17.2641$ Å [$M(10) = 23$].³¹ These values are very similar to those of the trihydrate compound, showing that the structure likely rearranges itself with higher symmetry when a water

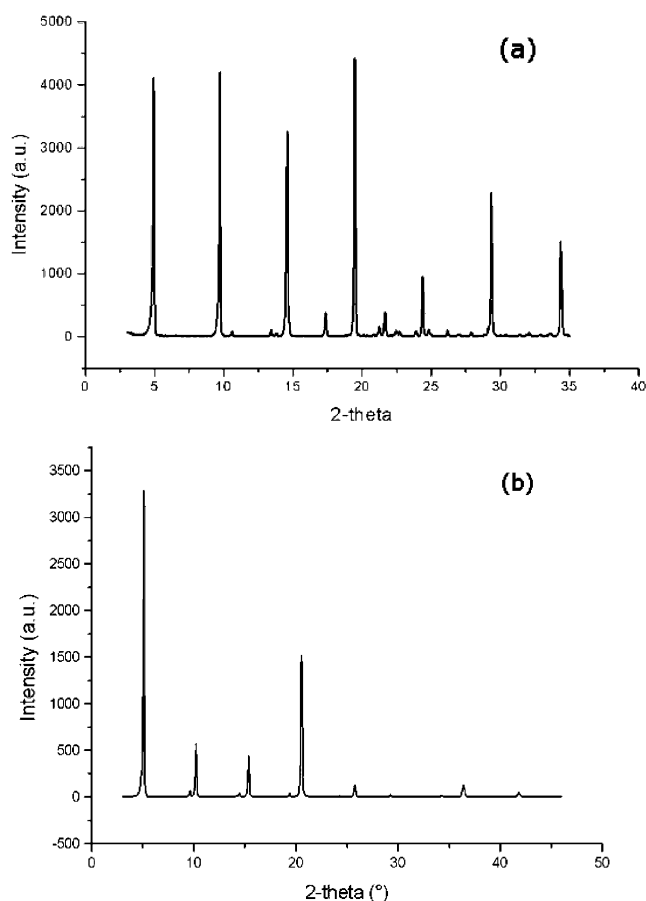


Figure 2. X-ray powder diffractograms for (a) $[\text{Cu(pcp)(H}_2\text{O)}_2]\cdot\text{H}_2\text{O}$ and (b) $[\text{Cu(pcp)(H}_2\text{O)}_2]$.

Table 3. Selected Bond Lengths and Angles for **1**

Bond Lengths (Å)			
Cu(1)—O(3)	1.933(5)	P(1)—C(1)	1.809(9)
Cu(1)—O(1)	1.962(5)	P(1)—C(11)	1.823(10)
Cu(1)—O(2) ^a	1.986(5)	P(2)—O(4)	1.494(6)
Cu(1)—O(6)	1.991(6)	P(2)—O(3)	1.516(5)
Cu(1)—O(5)	2.215(6)	P(2)—C(1)	1.795(9)
P(1)—O(1)	1.507(6)	P(2)—C(21)	1.811(9)
P(1)—O(2)	1.529(5)		
Bond Angles (deg)			
O(3)—Cu(1)—O(1)	92.8(2)	O(1)—P(1)—C(11)	108.5(4)
O(3)—Cu(1)—O(2) ^a	167.9(2)	O(2)—P(1)—C(11)	108.8(3)
O(1)—Cu(1)—O(2) ^a	89.3(2)	C(1)—P(1)—C(11)	108.1(4)
O(3)—Cu(1)—O(6)	85.8(2)	O(4)—P(2)—O(3)	115.8(3)
O(1)—Cu(1)—O(6)	165.6(3)	O(4)—P(2)—C(1)	109.6(4)
O(2) ^a —Cu(1)—O(6)	89.2(2)	O(3)—P(2)—C(1)	106.9(4)
O(3)—Cu(1)—O(5)	96.9(2)	O(4)—P(2)—C(21)	108.1(4)
O(1)—Cu(1)—O(5)	96.8(2)	O(3)—P(2)—C(21)	108.4(4)
O(2) ^a —Cu(1)—O(5)	94.7(2)	C(1)—P(2)—C(21)	107.8(4)
O(6)—Cu(1)—O(5)	97.7(3)	P(1)—O(1)—Cu(1)	133.4(4)
O(1)—P(1)—O(2)	113.9(3)	P(1)—O(2)—Cu(1) ^b	119.5(3)
O(1)—P(1)—C(1)	108.2(4)	P(2)—O(3)—Cu(1)	135.0(3)
O(2)—P(1)—C(1)	109.1(4)	P(2)—C(1)—P(1)	116.2(5)

^a Symmetry transformation ($x, -y, z + 1/2$) was used to generate equivalent atoms. ^b Symmetry transformation ($x, -y, z - 1/2$) was used to generate equivalent atoms.

molecule is lost. Unfortunately the attempts to solve this structure failed because of the presence of several impurity lines in the diffraction pattern. Concerning the material resulting from dehydration of $\text{Cu(pcp)(H}_2\text{O)}_2$, the XRD powder pattern did not show any peak, reflecting that the crystal structure collapsed and the sample became amorphous. A crystalline phase of the anhydrous Cu(pcp) , which does not react with water, has been successively isolated in hydrothermal conditions and the details of its structure, solved ab initio by XRPD and analogous to that of the reported 1D Pb(pcp) polymer,¹⁶ will be published.³²

The solid complex $[\text{Cu(pcp)(H}_2\text{O)}_2]\cdot\text{H}_2\text{O}$ easily reacts in water with stoichiometric amounts of bipy to give blue solutions. Evaporation of the water at 70–80°C affords well-shaped blue crystals of formula $[\text{Cu(pcp)(bipy)(H}_2\text{O)}]$.

The complexes **1** and **4** are paramagnetic with μ_{eff} of 1.93 μ_{B} and 1.90 μ_{B} , respectively, at room temperature. These values are consistent with noninteracting five-coordinated copper ions at room temperature.

Description of the Structures. As recently reported, all the complexes of the isomorphous series $[\text{M(pcp)(H}_2\text{O)}_3]\cdot\text{H}_2\text{O}$, where $\text{M} = \text{Ni(II), Co(II) and Mn(II)}$ (both mono and mixed), are isostructural, their structures being constituted by bidimensional layers. As a matter of fact polymeric chains, built up by an alternating array of metals centers and phenylphosphinate ligands, are connected through strong hydrogen-bonding linkages to form corrugated 2D layers.

An X-ray structural determination of $[\text{Cu(pcp)(H}_2\text{O)}_2]\cdot\text{H}_2\text{O}$ revealed again a 2D layered structure but differing from the above series in the number of coordination waters (Table 3 reports selected bond distances and angles). Now the metal center is five-coordinated, being surrounded by three phos-

(29) Zhang, Y.; Scott, K. J.; Clearfield, A. *Chem Mater.* **1993**, *5*, 495.

(30) Werner, P. E.; Eriksson, L.; Westdhal, M. *J. Appl. Crystallogr.* **1985**, *18*, 367.

(31) De Wolff, P. M. *J. Appl. Crystallogr.* **1968**, *1*, 108.

(32) Costantino, F.; Midollini, S.; Orlandini, A. Unpublished results.

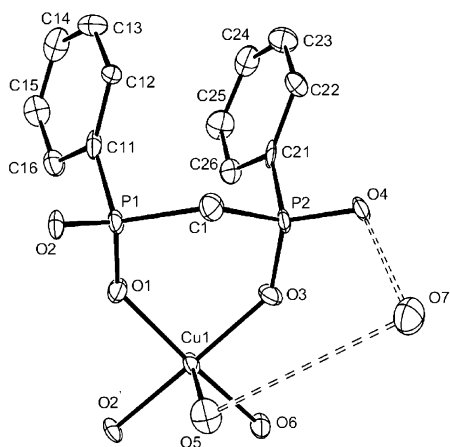


Figure 3. Perspective view of the asymmetric unit of the polymer $[Cu(pcp)(H_2O)_2] \cdot H_2O$: ORTEP III drawing with 30% probability ellipsoids.

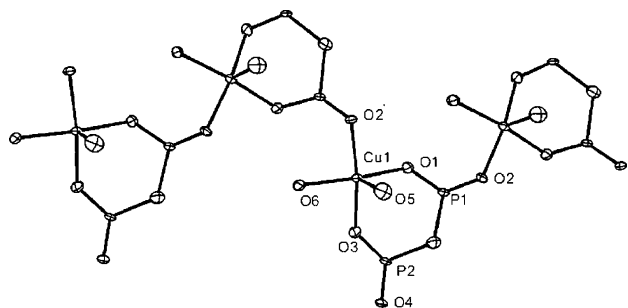


Figure 4. Perspective view of some symmetry-related units of $[Cu(pcp)(H_2O)_2] \cdot H_2O$ showing the zigzag chain propagated along the z axis. Phenyl rings are omitted for the sake of clarity.

phinate oxygen atoms from two ligands (one of them in bidentate and the other in monodentate fashion) and by two water molecules. The geometry is distorted square pyramidal, with the basal sites occupied by the phosphinate oxygen atoms and by a water molecule, with the metal displaced 0.22 Å above the basal plane. The third water molecule is present as a solvating moiety (see Figure 3). An alternating array of CuO_5 copper moieties and bridging phosphinate ligands creates an infinite zigzag chain, where the $Cu \cdots Cu$ separation is 5.36 Å (see Figure 4). Very important is the role played by the water molecules, both of coordination and of crystallization, in the building up of the structure. As a matter of fact an extended net of hydrogen bonding connects the chains together, resulting in a corrugated 2D layer (see Figure 5). The most important linkages are displayed by the solvating water molecule (O7), which, through hydrogen-bonding interaction with itself, creates an infinite winding of water molecules between the chains [$O7 \cdots O7^I$ 2.77 Å (I $1 - x, -1 - y, -z$); $O7 \cdots O7^{II}$ 2.81 Å (II $1 - x, y, -0.5 - z$)]. These water molecules are in turn connected through hydrogen bonding to the water oxygen (O5) coordinated to the metal and to the phosphinate oxygen (O4) not involved in direct bond to the copper [$O7 \cdots O5^I$ 2.75 Å (I $1 - x, -1 - y, -z$); $O7 \cdots O4$ 2.69 Å]. Another very important interchain hydrogen-bonding interaction is due to the same phosphinate oxygen O4 with the coordinated water oxygen O6 [$O4 \cdots O6^{III}$ 2.68 Å (III $x, -1 - y, -0.5 + z$)]. Other intrachain interactions < 3.0 Å, even if of minor importance, are present in the lattice and are anyway significant in the

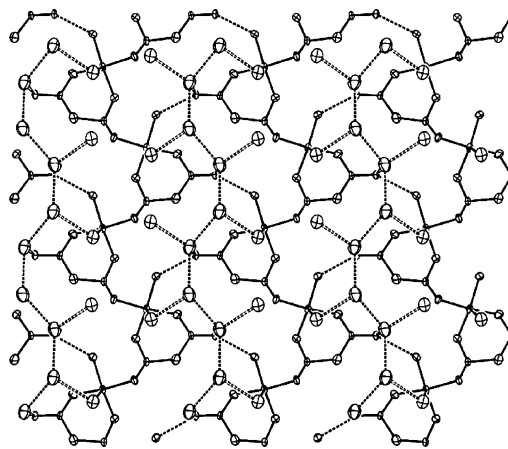


Figure 5. Perspective view of a portion of the polymer $[Cu(pcp)(H_2O)_2] \cdot H_2O$, showing the propagation of the layer in the yz plane. For the sake of clarity, the phenyl rings are omitted and only the most important interchain hydrogen-bonding connections are represented.

cementing of the whole architecture [$O1 \cdots O6^{IV}$ 2.76 Å (IV $x, -y, -0.5 + z$); $O2 \cdots O6^{IV}$ 2.79 Å; $O2 \cdots O5^{II}$ 2.92 Å]. The extension of the structure in the third dimension is precluded by the presence of the organic part of the hybrid ligand, which through the phenyl rings shields each other from the 2D layers. The packing diagram of the above polymer with view normal to $[010]$ is given in Figure 6.

Bond distances and angles in the coordination polyhedron of the copper center are as expected, the $Cu-O$ in the basal plane being significantly shorter [average 1.97(1) Å] than the $Cu-O$ in apical position [2.215(6) Å]. The values of the $P-O$ distance lie in a range 1.494(6)–1.529(5) Å and the $O-P-O$ angles are slightly larger than the tetrahedral, probably because of the involvement of oxygen in the bridge formation.

The structure of **4** consists of monodimensional $[Cu(pcp)(bipy)(H_2O)]$ hydrogen-bonding polymers. In the asymmetric unit the copper center is surrounded in a distorted square pyramidal geometry by two phosphinate oxygen donors, two bipy nitrogen atoms, and one water molecule in the apical position (see Figure 7). Table 4 reports selected bond distances and angles of **4**. The copper lies 0.26 Å above the basal plane. Unlike the structure of **1**, here the ligand phenylphosphinate coordinates as bidentate only one metal center, so that two phenylphosphinate oxygen atoms remain free and available for hydrogen-bonding interactions with the water molecule of one neighboring moiety. It results in an infinite chain, where phenylphosphinate ligands are bridging the metal centers through strong hydrogen bonding [$O2 \cdots O5^I$ 2.72 Å; $O4 \cdots O5^I$ 2.72 Å (I $1 + x, y, z$)] (see Figure 8). The inorganic part of each chain is shielded by a hydrophobic region, namely, by the phenyl rings of the pcp ligand and the bipyridine molecules. In the lattice the chains are packed in pairs, so that two chains, facing each other with the bipy ligand, create a column where the bipy planes are stacked, with a slightly alternate sliding (the shortest contacts between the atoms of two adjacent bipy moieties of ca. 3.5 Å are likely indicative of some stabilizing $\pi-\pi$ interactions). Interestingly the open site in the coordination sphere of the metal is directed toward one ring of the bipy

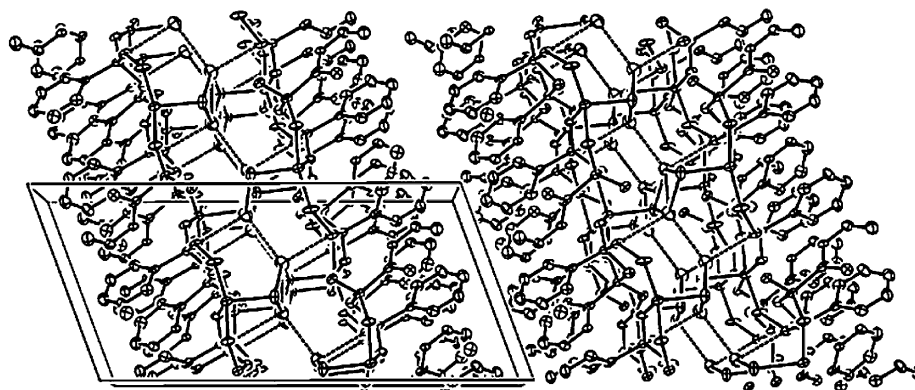


Figure 6. Packing diagram of $[\text{Cu}(\text{pcp})(\text{H}_2\text{O})_2]\cdot\text{H}_2\text{O}$, with view normal to $[010]$.

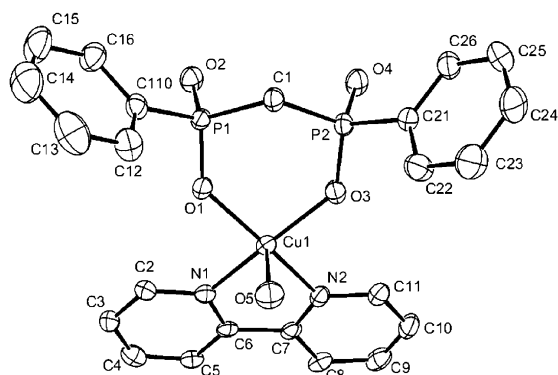


Figure 7. Perspective view of the asymmetric unit of $[\text{Cu}(\text{pcp})(\text{bipy})](\text{H}_2\text{O})$: ORTEP III drawing with 30% probability ellipsoids.

Table 4. Selected Bond Lengths and Angles for 4

Bond Lengths (Å)			
Cu(1)–O(1)	1.931(3)	P(2)–O(4)	1.495(4)
Cu(1)–O(3)	1.939(3)	P(2)–O(3)	1.512(3)
Cu(1)–N(1)	2.010(4)	P(2)–C(21)	1.801(4)
Cu(1)–N(2)	2.016(4)	P(2)–C(1)	1.810(5)
Cu(1)–O(5)	2.174(4)	N(1)–C(2)	1.341(6)
P(1)–O(2)	1.484(4)	N(1)–C(6)	1.347(6)
P(1)–O(1)	1.511(3)	N(2)–C(11)	1.340(6)
P(1)–C(110)	1.800(5)	N(2)–C(7)	1.351(5)
P(1)–C(1)	1.803(4)	C(6)–C(7)	1.479(6)
Bond Angles (deg)			
O(1)–Cu(1)–O(3)	96.54(14)	O(4)–P(2)–O(3)	117.3(2)
O(1)–Cu(1)–N(1)	89.51(14)	O(4)–P(2)–C(21)	109.4(2)
O(3)–Cu(1)–N(1)	163.68(14)	O(3)–P(2)–C(21)	106.9(2)
O(1)–Cu(1)–N(2)	161.72(14)	O(4)–P(2)–C(1)	111.6(2)
O(3)–Cu(1)–N(2)	89.99(14)	O(3)–P(2)–C(1)	107.3(2)
N(1)–Cu(1)–N(2)	79.98(15)	C(21)–P(2)–C(1)	103.3(2)
O(1)–Cu(1)–O(5)	94.89(17)	P(1)–O(1)–Cu(1)	134.3(2)
O(3)–Cu(1)–O(5)	94.20(17)	P(2)–O(3)–Cu(1)	135.2(2)
N(1)–Cu(1)–O(5)	100.39(16)	C(2)–N(1)–C(6)	118.6(4)
N(2)–Cu(1)–O(5)	101.66(17)	C(2)–N(1)–Cu(1)	125.6(3)
O(2)–P(1)–O(1)	116.3(2)	C(6)–N(1)–Cu(1)	115.7(3)
O(2)–P(1)–C(110)	109.7(2)	C(11)–N(2)–C(7)	118.8(4)
O(1)–P(1)–C(110)	106.1(2)	C(11)–N(2)–Cu(1)	125.5(3)
O(2)–P(1)–C(1)	111.2(2)	C(7)–N(2)–Cu(1)	115.6(3)
O(1)–P(1)–C(1)	107.3(2)	P(1)–C(1)–P(2)	115.9(3)
C(110)–P(1)–C(1)	105.5(2)	N(1)–C(6)–C(7)	114.4(4)
		N(2)–C(7)–C(6)	114.1(4)

of the neighboring chain. No important interaction involving the metal seems anyway present. In Figure 9 the packing diagram of **4** with view normal to $[100]$ is reported.

From a comparison of the coordination spheres of **4** and **1**, a larger distortion of **4** is evidenced by the axial angles of the square pyramid of 161.7° and 163.7° vs 165.6° and

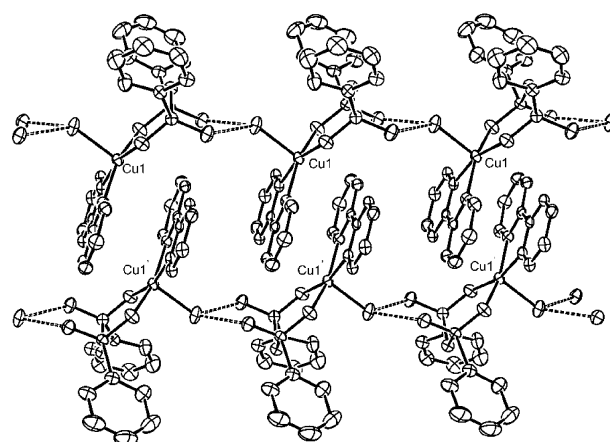


Figure 8. Perspective view of some symmetry-related units of $[\text{Cu}(\text{pcp})(\text{bipy})](\text{H}_2\text{O})$, showing the propagation of the chains in the x direction.

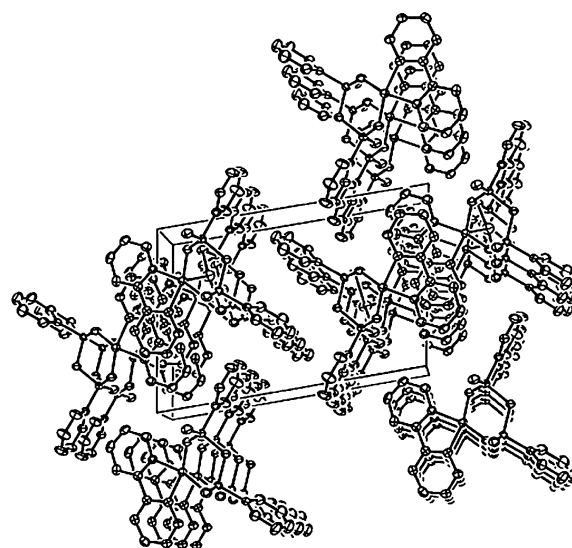


Figure 9. Packing diagram of $[\text{Cu}(\text{pcp})(\text{bipy})](\text{H}_2\text{O})$ with view normal to $[100]$.

167.9° in **1**. As in **1**, the apical bond distance [$2.174(4)$ Å] is significantly larger than the basal ones [the Cu–O and Cu–N linkages average $1.935(4)$ and $2.013(3)$ Å, respectively].

Thermogravimetric Study. The removal of water molecules could represent an important challenge, to leave open coordination sites on the metals for possible intercalation or catalytic reactions. With this kept in mind, an extensive

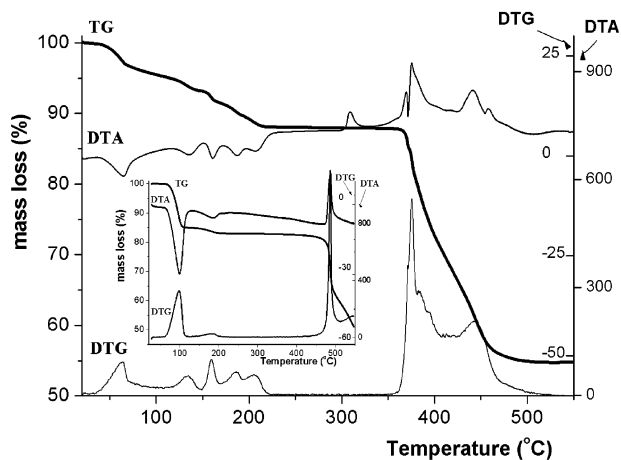


Figure 10. TG/DTG–DTA curves of $[Cu(pcp)(H_2O)_2] \cdot H_2O$. (Insets) TG/DTG–DTA curves for the isomorphous series member $[Ni(pcp)(H_2O)_3] \cdot H_2O$. TG = mass loss (percent); DTA = ΔT (microvolts) and DTG = percent per minute (\downarrow endo and \uparrow exo).

Table 5. Thermal Data of the Dehydration Process for All Samples

complexes	ΔT (°C)	$N^{\circ}H_2O$ losses	calcd/found (%)
$[Cu(pcp)(H_2O)_2] \cdot H_2O$ 1	25–202	2.9	13.11/12.54
$[Ni(pcp)(H_2O)_3] \cdot H_2O$	27–210	4.0	16.94/17.00
$[Mn(pcp)(H_2O)_3] \cdot H_2O$	33–139	4.0	16.94/17.00
$[Co(pcp)(H_2O)_3] \cdot H_2O$	29–128	4.0	16.94/17.00
$[Cu(pcp)(H_2O)_2]$ 2	27–200	2.0	9.14/9.14
$[Cu(pcp)(H_2O)]$ 3	26–221	1.1	4.79/5.26
$[Cu(pcp)(bipy)(H_2O)]$ 4	30–197	1.1	3.38/3.63

thermogravimetric study has been performed on the copper derivatives $[Cu(pcp)(H_2O)_2] \cdot H_2O$, $[Cu(pcp)(H_2O)_2]$, $[Cu(pcp)(H_2O)]$, and $[Cu(pcp)(bipy)(H_2O)]$ and on the related compounds of the isomorphous series $[M(II)(pcp)(H_2O)_3] \cdot H_2O$ [where $M(II) = Ni, Mn, \text{ and } Co$]¹⁴ for comparison purposes. Thermal data of the dehydration process for all samples are reported in Table 5.

The thermal behavior of $[Cu(pcp)(H_2O)_2] \cdot H_2O$ **1** (Figure 10 and Table 5) shows, from 25 to 202 °C, a complicated first weight loss with five overlapped stages (see DTG curve), which is likely attributable to the loss of the water molecules. In fact, the temperature range is in agreement with previous reports¹³ and the total loss of mass in this process corresponds to ca. three water molecules (calcd 13.11% vs found 12.54%). The water loss begins at relatively low temperature according to the preparative experiments. It is noteworthy that, during the process, the crystallization water molecules are not distinguished from the coordination ones. This fact could well be justified because in the crystal structure the water molecules are strongly involved in a complicated hydrogen-bonding network and anchored to the structural building. It is interesting to note that at ca. 150 °C the loss of weight corresponds to ca. two water molecules, in agreement with the preparative experiment.

Accordingly, the curves of the complex $[Ni(II)(pcp)(H_2O)_3] \cdot H_2O$, an example of the isomorphous series (see inset in Figure 10), substantially show that, during the heating, the complex loses the crystallization water molecule, followed by the coordinated ones in two overlap steps (see DTG curve). Also in this case the involvement of the water molecules in an extended hydrogen-bonding network can

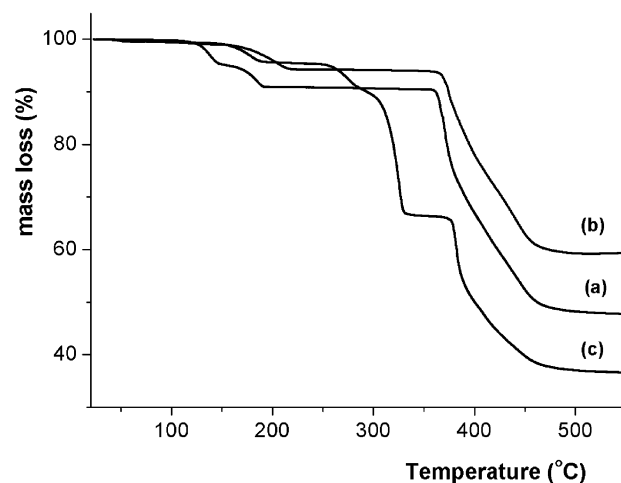


Figure 11. TG curves of (a) $[Cu(pcp)(H_2O)_2]$ **2**, (b) $[Cu(pcp)(H_2O)]$ **3**, and (c) $[Cu(pcp)(bipy)(H_2O)]$ **4**. TG = mass loss (percent).

justify the step overlapping.^{13,14} The corresponding curves of the Mn(II) and Co(II) derivatives, reported in the Supporting Information, appear quite similar. On the other hand, the first strong DTA peak temperature for the removal of the water molecules follows the order Mn(II) (69 °C) < Co(II) (78 °C) < Ni(II) (99 °C), indicating decreasing acidity from Mn(II) to Ni(II).

The thermal behavior for **2–4** in the water evaporation range of temperature (<300 °C) appears comparatively simple (Figure 11). Thus, compound **2** (curve a) shows two overlapped weight losses; the first at 155 °C [(DTG)_{peak} at 138 °C (one water molecule)] and the second at 200 °C [(DTG)_{peak} at 185 °C (one water molecule)] with endothermic associated processes [(DTA)_{peak} at 141 and 187 °C]. Analogously, compounds **3** and **4** (curves b and c) show respectively one loss of weight at 221 °C [(DTA)_{peak} at 207 °C] and one at 197 °C [(DTA)_{peak} at 178 °C], each corresponding to ca. one water molecule. Since compound **4** has been ascertained by X-ray crystal structure (see above) to contain one coordination water molecule, we can trustfully assign also the water molecules in **2** and **3** as metal-coordinated.

After the dehydration steps, there is a region of constant weight at high temperature for all the compounds. The existence of exothermic peaks [(DTA)_{peak} at 309, 305, and 312 °C for **1**, **2**, and **3**, respectively] is due to a possible phase transition followed by a strong exothermic effect, caused by the combustion of part of the organic matter. The IR spectrum (reported in the Supporting Information) shows that actually the bands due to the $\nu_{(OH)}$ vibrations of the water molecules are not present. This behavior is closely related to that of the recently reported, anhydrous derivatives $[M(II)(pcp)]$, where $M(II) = Zn \text{ or } Pb$.¹⁵

Summary

In accord with previous reports, diphenylmethylenediphosphinate is a suitable ligand to produce extended materials with metal(II) ions.^{13–16,32} We have now found that the heating of aqueous solutions of H_2pcp and copper(II) ions allows the formation of two different hydrated polymeric compounds: $[Cu(pcp)(H_2O)_2] \cdot H_2O$ and $[Cu(pcp)(H_2O)_2]$.

The structure of $[\text{Cu}(\text{pcp})(\text{H}_2\text{O})_2]\cdot\text{H}_2\text{O}$ consists of an alternating array of CuO_5 copper moieties and bridging diphosphinates resulting in infinite zigzag chains. These are connected together by an extended net of hydrogen bonding to give a corrugated 2D layer. Hydrogen bonds are formed by both the coordinating and crystallization water molecules, and the solvating water plays a determining role in the construction of the crystal packing. The determinant cementing role of the solvating water molecules is in agreement with the thermal analysis results, where the presence of only one complicated dehydration step seems due to the difficulty in distinguishing the loss of crystallization water from that of coordinated water. Consistently the two compounds **1** and **2**, despite the close formulas, have different lattices, and they cannot be interconverted by a direct reaction. The complex **1** easily loses two water molecules to form a new derivative of formula $[\text{Cu}(\text{pcp})(\text{H}_2\text{O})]$. This latter, even if not more crystalline, retains the primary structure because it can be quantitatively reconverted into **1** in the presence of water. This property, typical of open-framework materials, suggests a potential involvement of these phosphinate hybrids in the field of the intercalation chemistry and/or catalytic processes.

The easy substitution of the water molecules in **1** is evidenced also by the formation of the bipy derivative **4**. In the latter complex, the coordination of a diamine to the copper ion leads the diphosphinate ligand to coordinate as bidentate only one metal center. It ensues a hydrogen-bonding monodimensional polymer, where the non-metal-bonded phenylphosphinate oxygens are involved in strong hydrogen-bonding interactions with the water molecule of one neighboring moiety.

Acknowledgment. We thank Dr. S. Costantini (Università di Firenze) for microanalyses and Mr. F. Cecconi (ICCOM, CNR) for the synthesis of the ligand.

Supporting Information Available: Thermogravimetric curves for $[\text{Mn}(\text{pcp})(\text{H}_2\text{O})_3]\cdot\text{H}_2\text{O}$ and $[\text{Co}(\text{pcp})(\text{H}_2\text{O})_3]\cdot\text{H}_2\text{O}$ and FTIR of $[\text{Cu}(\text{pcp})(\text{H}_2\text{O})_2]\cdot\text{H}_2\text{O}$ at high temperatures (PDF). This information is available free of charge via the Internet at <http://pubs.acs.org>. Crystallographic data for structures **1** and **2** in CIF format have been deposited with the Cambridge Crystallographic Data Centre, nos. CCDC 249822 and 249823, respectively.

IC050171A